ABSORPTION AT ELECTRON CYCLOTRON RESONANCE IN SLIGHTLY IONIZED GASES (III)*

BY

Shigetoshi TANAKA

(Received March 17, 1961)

ABSTRACT

It was verified by measuring the loss in a slightly ionized gas $(\eta \lesssim 0.2)$ that the absorption curve at electron cyclotron resonance for the hybrid wave $(k_0 \perp B)$ is well represented by the expression which was previously derived. It was shown that the electron density and the collision frequency are determined from the resonance position and the half-width of one measured absorption curve. The collision probabilities in neon, argon and helium plasmas were determined from the pressure dependence of the collision frequency which was somewhat larger than those reported by other authors.

1. Introduction

In the second part of this paper**, an expression representing the cyclotron resonance absorption of electrons in a slightly ionized gas was derived for the hybrid wave $(k_0 \perp B)$. And it was shown that the resonance occurs at $\omega_c = \sqrt{\omega^2 - \omega_p^2 - \nu_c^2}$ and the absorption curve is not Lorentzian and the half-width depends on the collision frequency and the electron density.

In this part, it has been verified from the experimental studies that the absorption curve for the hybrid wave in dilute plasmas $(\eta \lesssim 0.2)$ is given by (6) of II. Accordingly, the electron density and the collision frequency are determined from the resonance position and the half-width of one measured absorption curve***. In addition, collision probabilities in neon, argon and helium plasmas were determined from the pressure dependence of the collision frequency.

For the purely transversal wave $(k_0 /\!/ B)$, the theoretical and the experimental studies on the absorption at the electron cyclotron resonance were reported by Brown *et al.* (**2, 3**) and Goldstein *et al.* (**4**). For the hybrid wave $(k_0 \perp B)$, however, there have been very few reports on the resonance absorption. Schneider

---

* Reported in Japanese in "Kakuyugo Kenkyu (Nuclear Fusion Research)" 5 (Sept. 1960), 283.
** The preceding paper (Part II), referred to as II.
*** This procedure is very similar to the effective mass and the collision frequency being determined from the resonance position and the half-width of the cyclotron resonance of electron and hole in semiconductor (**1**). It is to be noted, however, that the similarity is superficial and the effective mass is not considered in the gaseous plasma.

et al. (5) carried out such experiments on the acetylene flame plasma, but they gave no comment on the shift of the resonance position. Recently, Mitani *et al.* (6), Dodo (7) and Yabumoto (8) have respectively found that the resonance position shifts with increasing electron density.

2. Experimental apparatus

The microwave power absorbed by a slightly ionized gas in a static magnetic field was measured with the apparatus shown in Fig. 1. The gaseous discharge plasma is maintained by D. C. power supply. The micowave (frequency $f_s = 9,820$ mc/s) modulated by $5\,kc/s$ square wave, after passing through the plasma-filled guide and a calibrated attenuator, is detected by a crystal detector. The detected signal is amplified by a selective amplifier and then displayed on an oscillograph. The insertion loss of the plasma is substituted by the calibrated attenuator being adjusted. At the fixed signal frequency, the attenuation factor αD at arbitrary tube current and magnetic field is measured, where α is the attenuation constant and D the effective path length of plasma for the microwave. In order to exclude
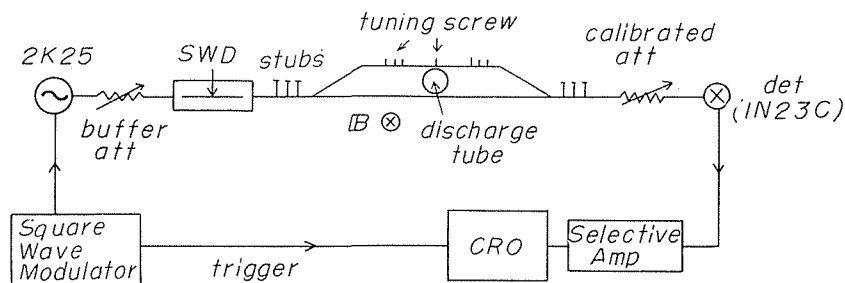

Fig. 1. Block diagram of the apparatus.

the disturbance due to Hall effect, the discharge current is set to be parallel to the magnetic field. In Fig. 2 is shown the magnet. The pole pieces have holes to get a discharge tube inserted, and are so shaped as to collect magnetic flux uniformly in the discharge tube. The discharge tube is in part within a waveguide running perpendicular to it. The waveguide is square and has a side equal to the longer side of standard X–band guides, which are connected through tapered parts to it. The details of the discharge tube relative to a vacuum and gas filling system are given in Fig. 3. A double probe is attached to the tube, outside the magnet. It is to be noted that the electron temperature and density measured by the probe are those in the case of no magnetic field.
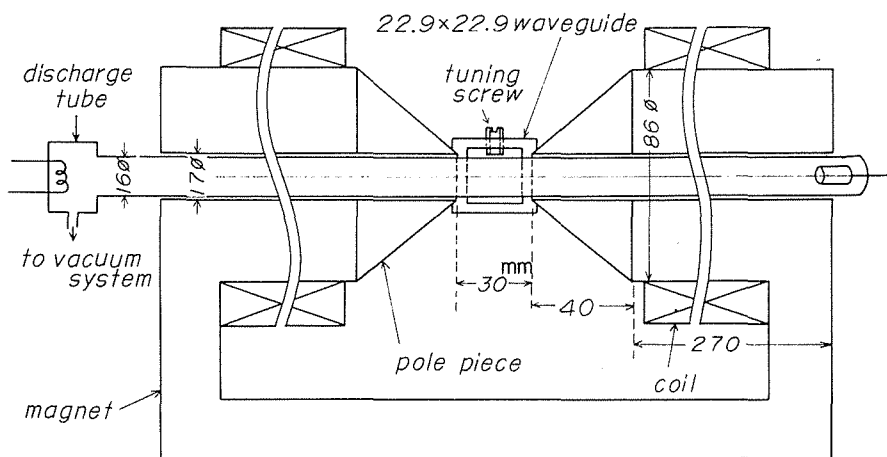
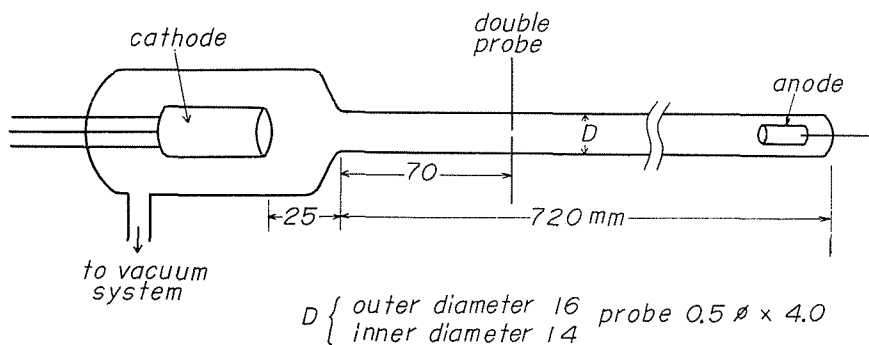Fig. 2. Waveguide connected with gaseous discharge tube and magnet.

$D \begin{cases} \text{outer diameter } 16 \\ \text{inner diameter } 14 \end{cases} \text{probe } 0.5 \varnothing \times 4.0$

Fig. 3. Discharge tube.

3. Experimental results

Experiments were made on the cyclotron resonance in gaseous discharge plasmas of neon, argon and helium. The neon plasma exhibited a sharp and typical resonance absorption in comparison with other plasmas. Therefore the experiments were performed mainly on the neon plasmas.

In Fig. 4 are shown the absorption (α) curves for the various discharge currents at constant pressure, plotted against magnetic field intensity B and $\gamma = \omega_c/\omega$, assuming the effective plasma length to be constant and the loss zero at far off-resonance positions, since it is negligibly small there. The values of $\eta = (\omega_p/\omega)^2$ and $\beta = \nu_c/\omega$ calculated from the absorption curves are given (see §4). Since p, hence ν_c is kept constant (assuming that collisions between electrons and neutral particles are dominant), these curves show how the resonance absorption varies
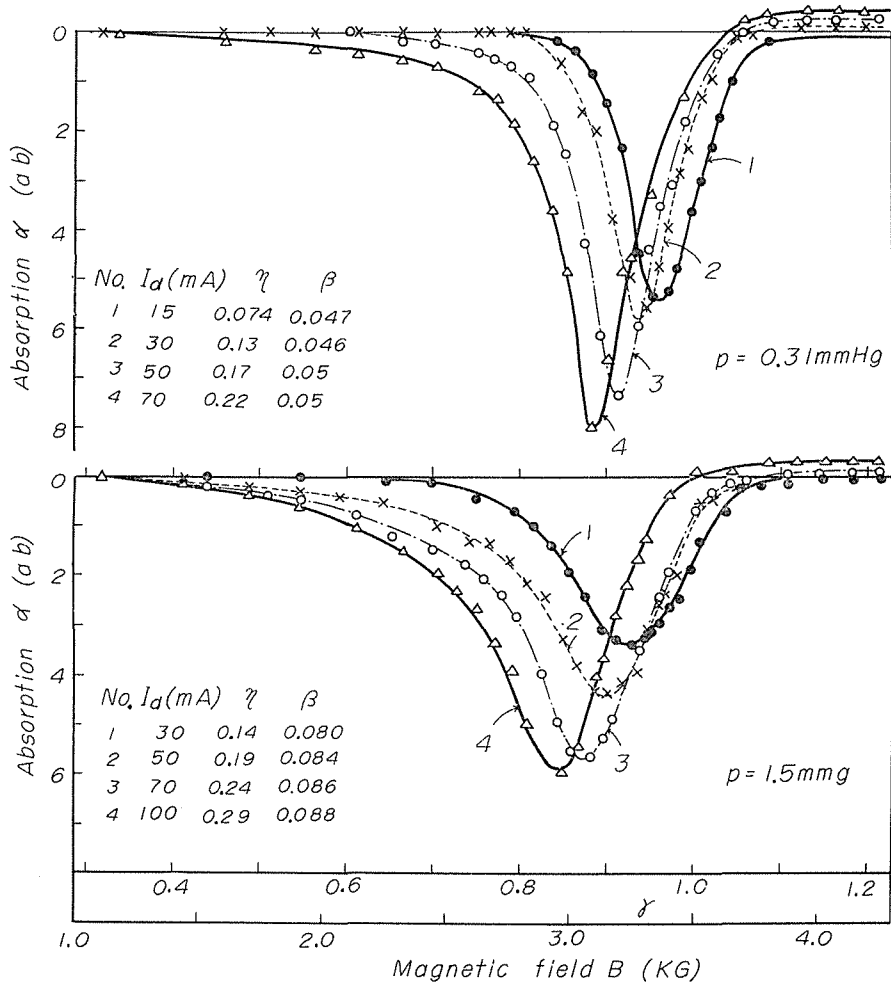
Fig. 4. Absorption curves for neon at constant pressure.

with increasing η and β=const..   Accordingly, these experimental curves directly correspond to the theoretical curves given in Fig. 4 of II.   In contrast to the previous curves, the absoption curves are shown in Fig. 5 for various values of p or β and I_d= const..   These curves show how the resonance absorption varies with increasing β and η=const..   Therefore, these experimental curves correspond to the theoretical ones given in Fig. 5 of II.

Before discussing the results in detail, we shall consider the problems accompanying the experiment.
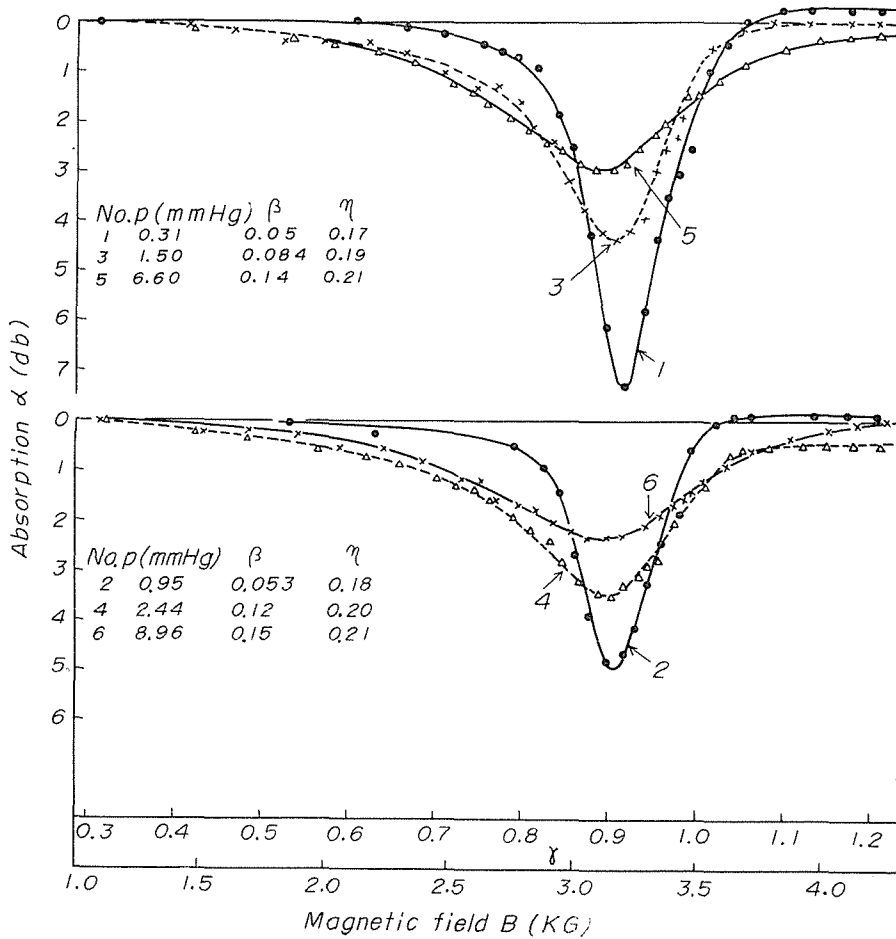
Fig. 5. Absorption curves for neon of constant discharge current ($I_d = 50$ mA.)

(1) *Leakage of microwave power*

If there is leakage of microwave power from two holes on guide walls, in which the discharge tube is set, the leaking wave will propagate in H_{11} mode through the holes in poles of magnet, as circular waveguides. On the other hand, the cutoff wavelength λ_c for such wave is given in the form (9):

$$\lambda_c = 2\pi a\sqrt{K_e}/\chi'_{11} = 2.9\sqrt{K_e} \quad \text{(cm)},$$

for the present case. Thus the signal wave ($\lambda = 3.05$ cm) is beyond the cutoff even if K_e is unity ($K_e < 1$ in a plasma), no leakage resulting.

(2) *Reflection of microwave from plasma*

Since the microwave power is measured after passing through the plasma, if

a large variation in reflection power from the plasma occurs in the vicinity of resonance, we shall observe an incorrect large absorption. Actually, the apparent absorption due to reflection at the resonance amounted to about $1\,db$, when the peak absorption due to plasma was $7.5\,db$. In order to avoid such errors, it is better that the matching to the plasma column is a little off, because a constant small reflection rather does not lead to error in our experiments.

(3) *Deformation of plasma column by magnetic field*

Setting discharge current parallel to magnetic field, we can exclude the disturbance due to Hall effect. However, the plasma is concentrated about the axis of the tube with magnetic field intensity being increased, due to the decrease in diffusion loss of electrons to the wall. In our experiments, the diameter of the intensely bright part became about one third of the inner diameter of the tube in the vicinity of resonance $(B \simeq 3.5\,KG)$. Although the effective path length of plasma for microwave varies by the deformation of plasma column, the experimental data cannot make correction for deformation.

(4) *Uniformity of magnetic field*

The magnetic field between the tapered pole pieces shown in Fig. 2 is not uniform, but the spatial variation of B within the plasma region is below about 3 percent, which may be negligible in our experiments.

(5) *Setting of zero-level of absorption curve*

We took the absorption to be zero at far off-resonance positions. Therefore, strictly the correct zero-level must be somewhat above those shown in Figs. 4 and 5. Moreover, the zelo-level at far off-resonance where $\gamma \ll \gamma_0$ does not correctly coincide with that where $\gamma \gg \gamma_0$. For convenience' sake, we took α to be zero at $\gamma \ll \gamma_0$.

(6) *Impurity gases*

In our experiments, impurity gases such as CO_2, CO, H_2O and N_2 which are emitted from oxide cathode, anode and tube wall at heating will broaden the absorption curve, since their collision probabilities are very large in comparison with sample gases*. So, they present a most troublesome problem.

---

* Under our experimental conditions in which the electron temperature is estimated to be $2 \sim 4 \times 10^4$ (°K), the collision probabilities of these gases are such as follows (**10**):

　　Ne: $7 \sim 8$ (cm-mmHg)$^{-1}$, Ar: $10 \sim 30$, He: 20, CO_2: $20 \sim 50$, CO: $50 \sim 120$, H_2O: $60 \sim 90$, N_2: $40 \sim 90$.

4. Discussion on experimental results

It was shown in II that for $\eta \ll 1$ the absorption curve can be approximated by :

$$\alpha_\perp = \alpha_{\perp m} \frac{\beta^2 (2-\eta)^2}{(\gamma_0^2 - \gamma^2)^2 + \beta^2 (2-\eta)^2} , \qquad (1)$$

with $\quad \alpha_{\perp m} = \dfrac{\pi \eta}{\beta} \dfrac{1-\eta}{2-\eta}$.

(1) Shift of resonance position and calculation of electron density

The resonance takes place at $\gamma = \gamma_0$, where

$$\gamma_0^2 = 1 - \eta - \beta^2 . \qquad (2)$$

In our experiments, β is 0.2 at most, so β^2 in (2) can be neglected against η. γ_0 is determined directly from the absorption curve and η by double probe respectively for various values of discharge current I_d. The experimental results together with the calculated values from (2) are shown in Fig. 6, where the experimental points are contained in respective blocks corresponding to different
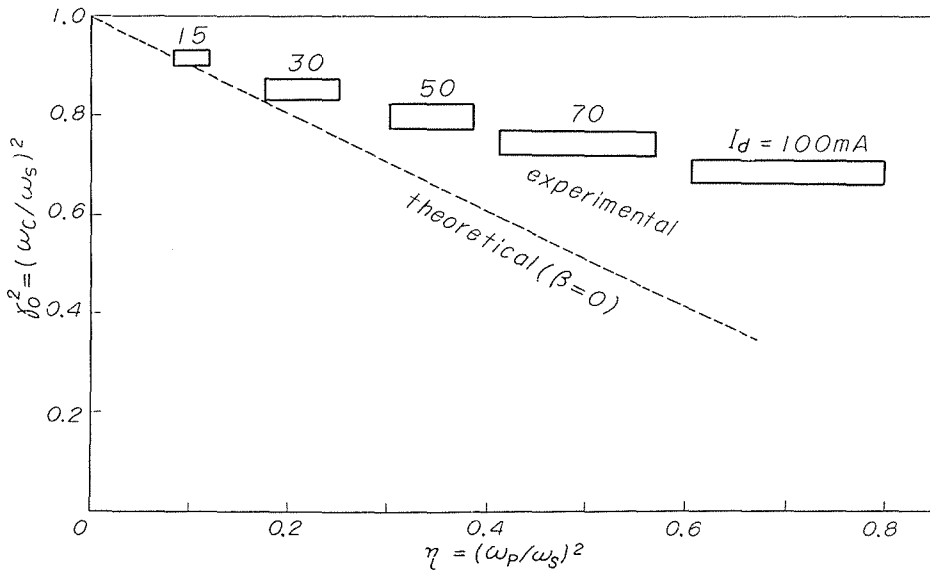
Fig. 6. Variation of reconance position γ_0^2 versus electron density η.

values of I_d. It seems to come from the circumstance that the electron density η may increase with increasing pressure as shown in Fig. 8, owing to the decrease of electron mobility. Obviously in Fig. 6, the experimental results agree with the theoretical ones in the domain $\eta \lesssim 0.2$ and $I_d \lesssim 30$ mA. A discrepancy occurs for

larger η, which is natural, since our theory given in (2) is correct only for small η. Thus, for small η, if $\tilde{\gamma}_0$ or the shift of the resonance position is measured,
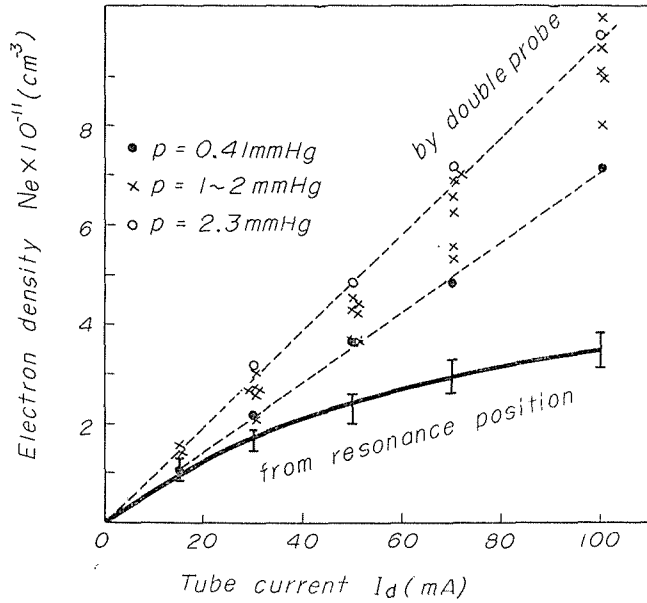

Fig. 7. Comparison between electron densities measured from resonance position and by double probe *versus* tube current.
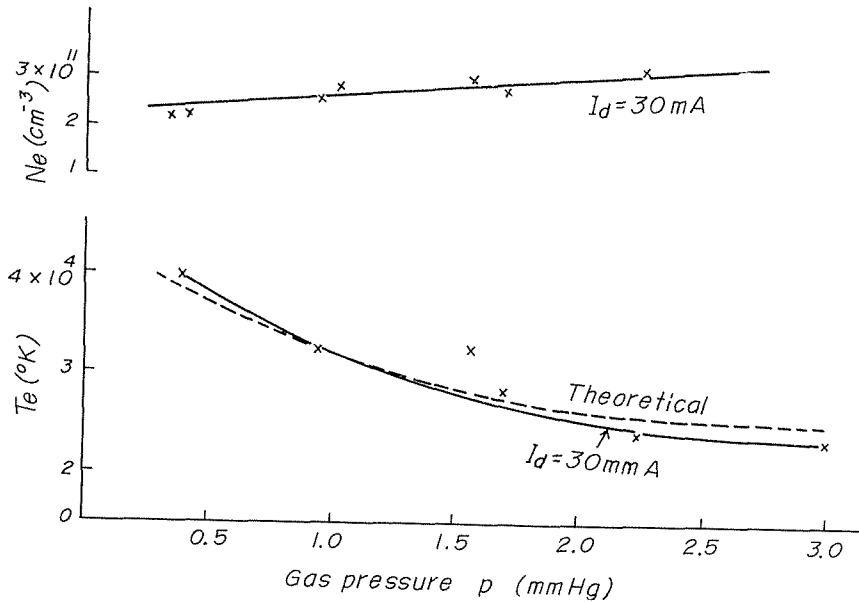

Fig. 8. Variation of T_e and N_e with p for neon.

we can easily calculate η, hence the electron density. In Fig. 7 are shown the electron densities (N_e) measured from resonance position and by double probe *versus* tube current. It is noted here that the electron density measured by probe is that in the case of no magnetic field.

In Fig. 8 are shown the electron density and the temperature (T_e) *versus* pressure which are calculated from double probe measurement according to Johnson-Malter (**11**) assuming $T_i = 400°\mathrm{K}$.

(2) *Asymmetry of absorption curves*

The absorption curve plotted against γ is not symmetrical and a measure of asymmetry is given by:

$$\frac{\Delta\gamma_-}{2} - \frac{\Delta\gamma_+}{2} \simeq \beta^2\left(1 + \frac{\eta}{2}\right), \tag{3}$$

as shown in II. Therefore, the absorption curve becomes more asymmetrical with increasing β than with increasing η, as it can in fact be seen from the experimental curves in Figs. 4 and 5.

According to (1), however, the absorption curves *versus* γ^2 is symmetrical. In Fig. 9 are plotted the experimental points together with the theoretical curves. Both agree well within the half-width but does not outside and this may be due to the way of setting the zero-level of absorption curve as stated in §3 (5).
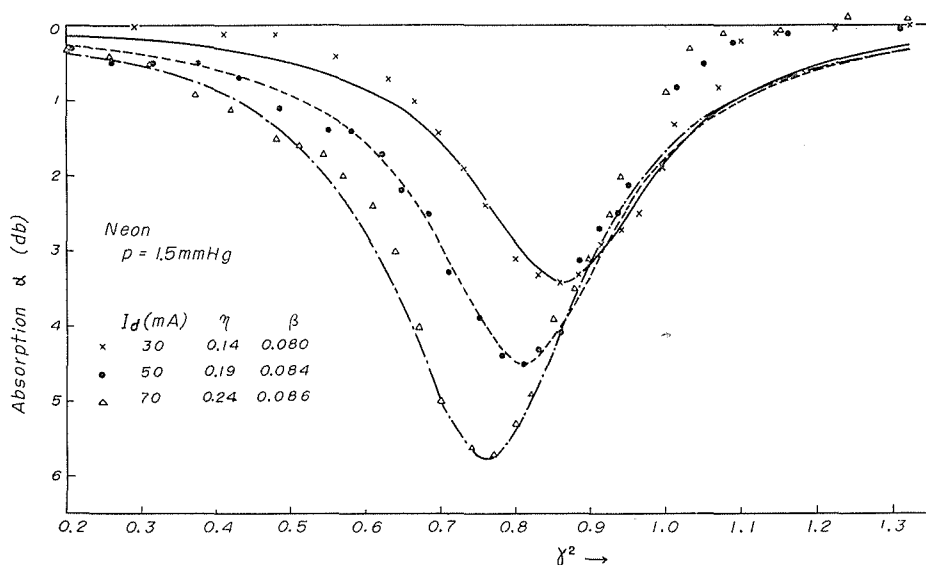

Fig. 9. Comparison between theory and experiment of resonance absorption *versus* γ^2.

(3) *Maximum absorption*

(a) Since $\alpha_{\perp m} = \{(1-\eta)/(2-\eta)\}\pi\eta/\beta$, we have

$$\alpha_{\perp m}\beta = \pi\eta(1-\eta)/(2-\eta) = \text{const.}, \qquad (4)$$

if $\eta = \text{const.}$. Therefore, $\alpha_{\perp m}$ is inversely proportional to β. Thus, as the pressure is increased with $I_d = \text{const.}$, the absorption peaks are lowered. From the experimental data at $I_d = 50\,\text{mA}$ given in Fig. 5, $\alpha_{\perp m}\beta$ are obtained as:

$$0.37,\ 0.27,\ 0.37,\ 0.42,\ 0.36.$$

(b) If $\beta = \text{const.}$, then

$$\frac{\alpha_{\perp m}}{\eta}\frac{2-\eta}{1-\eta} = \frac{\pi}{\beta} = \text{const.}, \qquad (5)$$

which implies that $\alpha_{\perp m}$ is very proportional to η. From the experimental data at $p = 1.5\,\text{mm Hg}$ given in Fig. 4, the values given on the left-hand side of (5) are 53, 53, 55, 50.

(4) *Half-width and collision probability*

The relation between the half-width and β is:

$$\Delta\gamma \simeq \left(2+\frac{\eta^2}{4}\right)\beta \quad \text{or} \quad \beta = \frac{1-\eta}{2-\eta}\frac{\Delta B}{B_0}, \qquad (6)$$

as shown in II. In Fig. 10 are shown the experimental data on β and ν_c *versus* p, which are obtained from the half-width.
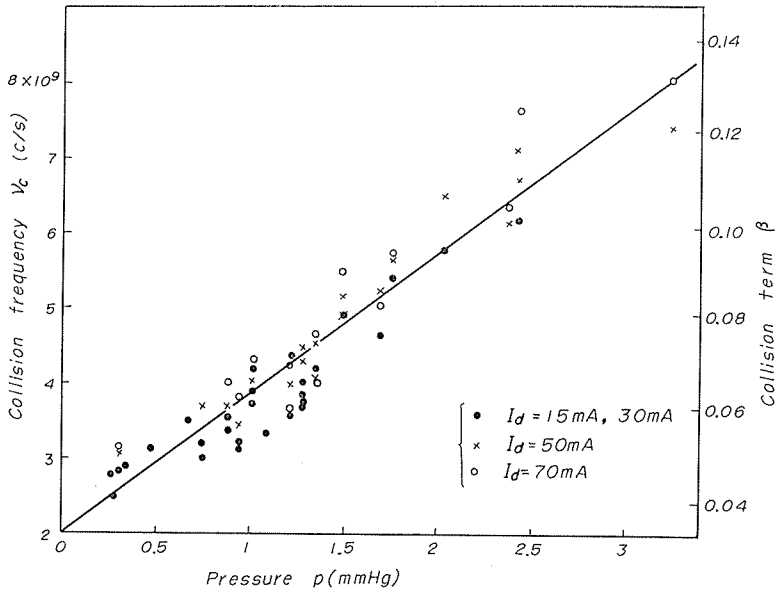

Fig. 10. Variation of collision frequency with pressure for neon,

On the other hand, ν_c is given by (12):

$$\nu_c = p_0 P_c V,\qquad\qquad(7)$$

where P_c is the collision probability, $p_0 = 273\, p/T_g$ the reduced pressure in mm Hg and V the average velocity of electron.

For neon, Ramsauer effect is very small and actually P_c can be taken as constant under our experimental conditions, in which the electron temperature varies from 4×10^4 to 2.3×10^4 °K, according to the pressure increase from 0.4 to 3 mm Hg as shown in Fig. 8. V varies by the factor $\sqrt{4/2.3} = 1.32$ in the above pressure range. If this variation of V can be neglected, ν_c depends only on p. From the experimental data in Fig. 10, this relation can be expressed approximately as:

$$\nu_c = 1.9 \times 10^9 p + 2.0 \times 10^9 \quad (c/s).\qquad\qquad(8)$$

The constant term independent of p in (8) is very difficult to be interpreted. However, in this case, the electron collisions with tube wall have been neglected in comparison with those with neutral particles, since the gyration radius of electron is about 2×10^{-2} mm even at $B = 3000$ gauss. The impurity gases emitted from electrode and wall, which are independent of p, may be responsible for this term. Such a constant term is seen in Whitmer's report (13), in which he has studied the electron loss process in hydrogen gas discharge with the microwave techniques.

From the pressure dependent term in (8), P_c is calculated as:

$$P_c = 25 \text{ cm}^2/\text{cm}^3 \text{ mm Hg},$$

where $T_g = 350$ °K and $T_e = 3 \times 10^4$ °K have been taken. This value of P_c is about three times larger than that reported (10). One of the reasons why such a large P_c is obtained is that the cyclotron resonance occurs at $\gamma_0^2 = 1 - \eta$, hence the spatial distribution of electron density of our experimental plasma causes naturally the absorption curves to be broadened. Also impurity gases may be responsible for such a large P_c.

5. Experimental results for argon

The experimental results of agron plasmas are similar to those of neon plasmas, except that the collision frequency is somewhat larger and the absorption curves broader. In Fig. 11 are plotted the experimental data on β and ν_c against p. Ramsauer effect of argon gas is very large and the collision probability varies from 12 to 5 cm²/cm³ mm Hg (10) as the electron temperature decreases from 2×10^4 °K to 1.25×10^4 °K, while the increase of the pressure from 0.5 to 5 mm Hg is accompanied by such a variation of electron temperature. But, neglecting the

Ramsauer effect and the variation of T_e, we assume that ν_c depends only on p, and ν_c can be expressed approximately from Fig. 11 as:

$$\nu_c = 1.4 \times 10^9 p + 4.0 \times 10^9 \quad (c/s). \tag{9}$$

Then, taking $T_g = 350\,°K$ and $T_e = 1.5 \times 10^4\,°K$, P_c is calculated as:

$$P_c \simeq 27\ \mathrm{cm^2/cm^3\ mm\ Hg},$$

which is rather larger than that reported (**10**).
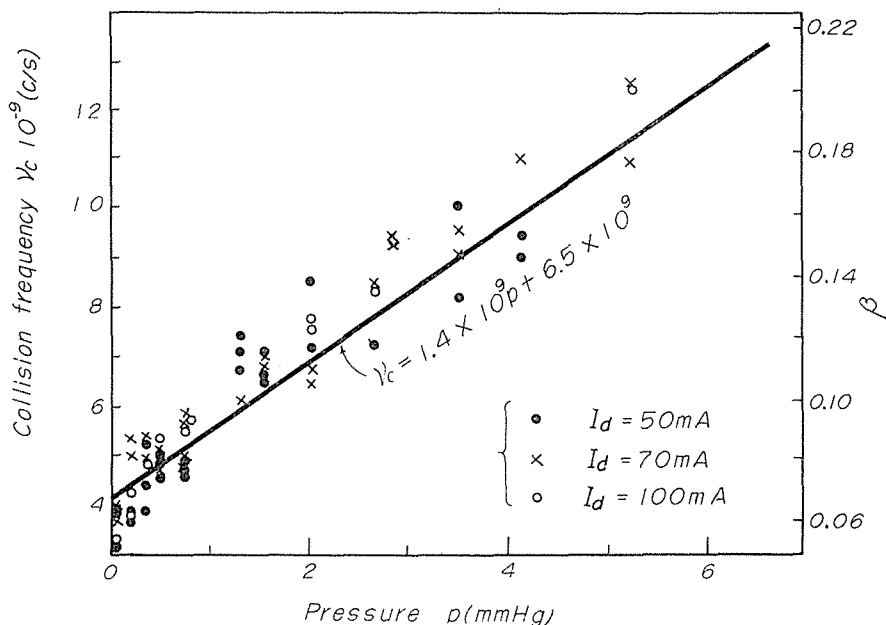

Fig. 11. Variation of collision frequency with pressure for argon.

6. Experimental results for helium

The absorption curves of helium plasma are similar to those of neon and argon, but they are very broad, since the electron temperature is high and the collision probability is large in helium gas. In Fig. 12 are plotted the experimental data on ν_c against p, which can be expressed as:

$$\nu_c = 1.4 \times 10^9 p + 6.5 \times 10^9 \quad (c/s). \tag{10}$$

Neglecting the variation of T_e from 4×10^4 to $3 \times 10^4\,°K$ as the pressure increases from 2.5 to 6 mm Hg, we can calculate P_c from (10), obtaining

$$P_c \simeq 18\ \mathrm{cm^2/cm^3\ mm\ Hg},$$

where $T_g = 350\ ^\circ K$ and $T_e = 3.5 \times 10^4\ ^\circ K$ have been taken. This value of P_c is consistent with that reported (**10**) ($P_c = 20$).
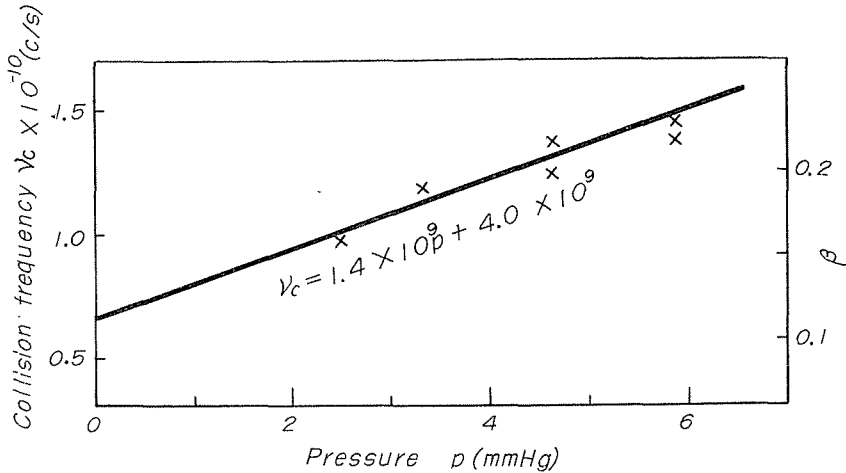

Fig. 12.   Variation of collision frequency with pressure for helium.

7.   Conclusion

It causes disadvantage for the hybrid wave to be used, that the absorption curve becomes rather complicated in comparison with that for the purely transversal wave, but it is meritorious that the electron density and the collision frequency are determined from the resonance position and the half-width. This circumstance can be applicable as microwave diagnostics to the studies of gaseous discharge plasmas.

Recently, Brown (**3**) has carried out the measurements on the cyclotron resonance radiation for the case of $k_0 \perp B$, and has shown that the resonance position shifts with increasing electron density. His result is consistent with ours if based on Kirchhoff's law. Schneider *et al.* (**5**) have carried out the measurements on the cyclotron resonance absorption for the case of $k_0 \perp B$, but wrongly discussed the result, using the absorption factor for $k_0 /\!\!/ B$. Practically, however, their results are not incorrect fortunately, because their measurements were made on very dilute plasmas ($\eta \approx 0.002$).

Finally, since there are boundaries to the test plasma generated in our laboratories, the effect of boundary must be considered, as considered in another report (**14**). Also, it will be necessary to consider the effect of long range Coulomb interaction (*e–i* and *e–e* collisions) and the effect of thermal energy of electrons and ions upon the electron cyclotron resonance.

Acknowledgments

In conclusion, the author wishes to express his sincere thanks to Prof. I. Takahashi for his guidance and to Prof. K. Mitani for his discussions. Thanks are also due to Prof. Y. Uchida and Dr. K. Fukuda for the convenience given to use electromagnet.

REFERENCES

1. G. DRESSELHAUS, A. F. KIP and C. KITTEL: Phys. Rev. **90** (1955), 368.
2. D. C. KELLY, H. MARGENAU and S. C. BROWN: Phys. Rev. **108** (1957), 1367.
3. S. C. BROWN: *Proc. of the 4th Intern. Conf. on Ionized Phenomena in Gases*, Uppsala, Aug., 1959 (IIIC 691).
4. L. GOLDSTEIN *et al.*: Technical Report No. 3 (1954) and Scientific Report No. 2 (1957), (University of Illinois).
5. J. SCHNEIDER and F. W. HOFFMAN: Phys. Rev. **116** (1959), 244.
6. K. MITANI and H. KUBO: (private communication).
7. T. DODO: (private communication).
8. T. YABUMOTO: (private communication).
9. N. MARCUVITZ: *Waveguide Handbook* (McGraw-Hill Co., Inc., 1951), p. 70.
10. S. C. BROWN: *Basic Data of Plasma Physics* (John Wiley & Sons, Inc., 1959) pp. 7~17.
11. E. O. JOHNSON and L. MALTER: Phys. Rev. **80** (1950), 58.
12. S. C. BROWN: ibid. p. 3.
13. R. F. WHITMER: Phys. Rev. **104** (1956), 572.
14. S. TANAKA: Kakuyugo Kenkyu (Nuclear Fusion Research) **5** (1960), 604 (in Japanese).